Математички Билтен
48 (LXXIV) 1 (2024), 40–52

UDC: 517.987.1:519.64
517.555.1:519.64
DOI: 10.37560/matbil2448140ak

NUMERICALLY VERIFYING THE ASSOUAD DIMENSION: THE SET $\{0\} \cup \{1/n : n \in \mathbb{N}\}$

JASMINA ANGELEVSKA KOSTADINOSKA

Abstract. In this case study, we aim to rigorously verify established theoretical properties concerning the Assouad dimension of the set $\{0\} \cup \{1/n : n \in \mathbb{N}\}$ through detailed calculations. This work serves as a foundational step towards identifying general principles governing the convergence behavior of Assouad dimension calculations for arbitrary fractals. Specifically, we investigate the necessary precision for the generation and measurement of such sets to achieve a target accuracy in the estimation of their Assouad dimensions.

1. INTRODUCTION

The Assouad dimension provides a measure of the maximal relative scaling exponent for the number of sets needed to cover a neighborhood of a set.

Definition 1.1. *Let $F \subseteq \mathbb{R}^n$ and denote by $N_r(F)$ the minimum number of open sets with radius at most r required to cover F. The **Assouad dimension** of F is defined as*

$$\dim_A F = \inf \Bigg\{ \alpha : \exists C > 0 \text{ such that } \text{for all } 0 < r < R,\ \sup_{x \in F} N_r(B(x,R) \cap F) \leq C \left(\frac{R}{r}\right)^{\alpha} \Bigg\} \quad (1.1)$$

where $B(x,R)$ is the open ball centered at x with radius R.

Despite its theoretical richness, practical applications of the Assouad dimension remain limited due to the complexity of its definition and the interdependence between scales R and r. Unlike the widely used box dimension (for definition see eg. [17]), which provides an "average" dimension over the entire set, the Assouad dimension emphasizes the most "fractured" parts of the set.

2010 *Mathematics Subject Classification.* Primary: 28A80, 65D99.
Key words and phrases. Assouad dimension, $\{0\} \cup \{1/n : n \in \mathbb{N}\}$, numerical analysis .

In the remainder of this paper, we let $F = \{0\} \cup \{1/n : n \in \mathbb{N}\}$. Whether F is a fractal or not in our interest. It is a discrete set with a structure that is interesting from the perspective of fractal geometry. Its significance lies in the theoretical exploration of dimensions, such as the Assouad dimension, which can reveal unique scaling behaviors even in sets that are not fractals in the traditional sense. While the following example is discussed in [11], we present it here for completeness and to facilitate subsequent calculations.

Example 1. *For $F = \{0\} \cup \{1/n : n \in \mathbb{N}\}$, we have $\dim_A F = 1$.*

Proof. To establish this, it suffices to find a constant $C > 0$, a sequence of points $x_n \in F$, and scales $0 < r_n < R_n$ such that $R_n/r_n \to \infty$ and for each n,

$$N_{r_n}(B(x_n, R_n) \cap F) \geq C\frac{R_n}{r_n}.$$

Let $x_n = 0$, $R_n = 1/n$, and $r_n = 1/n^2$ $\forall n \in \mathbb{N}$. For $k \geq n$, the distance between two consecutive points in the set is $\frac{1}{k} - \frac{1}{k+1} = \frac{1}{k(k+1)} < \frac{1}{n^2} = r_n$. Thus,

$$N_{r_n}(B(0, R_n)) \geq \frac{1}{2}n = 2^{-1}\left(\frac{R_n}{r_n}\right)^1.$$

□

The goal is to numerically estimate $\dim_A F$ with a specified precision. Drawing on techniques applied to other types of fractal dimensions, such as those in [17], we can transform the inequality

$$N_r(B(x, R) \cap F) \leq C\left(\frac{R}{r}\right)^\alpha$$

in Definition 1.1 to a logarithmic form:

$$\log N_r(B(x, R) \cap F) \leq \log C + \alpha \log\left(\frac{R}{r}\right).$$

Ideally, this allows us to determine α by calculating the slope of the line in a plot of $\log\left(\frac{R}{r}\right)$ versus $\log N_r(B(x, R) \cap F)$. This approach provides an effective means for estimating α by analyzing the linear relationship within this log-log plot.

Note: In Definition 1.1, we denote by $N_r(F)$ the minimum number of open sets with radius at most r required to cover F. For complex sets, determining the minimal cover is a nontrivial task. However, due to the simplicity of the set F in our case, this number can be calculated explicitly for given values of r and R.

This paper is organized as follows: in Section 2, we identify the challenges associated with the numerical estimation of the Assouad dimension for the set F. Section 3 presents the outcomes from our calculations. Finally, Section 4 offers a summary of our findings and concluding remarks.

2. CHALLENGES

2.1. **Generating the set.** The set F is infinite; however, for practical purposes, we approximate it by taking only the first N elements, resulting in a finite subset $F' = \{0\} \cup \{1/n : n \in \mathbb{N}, n \leq N-1\}$. Theoretically, this finite approximation F' has an Assouad dimension of $\dim_{\mathrm{A}} F' = 0$ regardless of the number of elements included.[1] By selecting an appropriate range and ratio for R and r, we observe a behavior that suggests an approximate exponential scaling, often referred to as the "window of fractality." This observation leads us to the following challenges:

2.2. **Ratio of R and r.** Generally, the parameters R and r can vary independently, but their interdependence is essential to capturing the Assouad dimension. If R and r vary freely, multiple regression analysis would be necessary to interpret their influence. However, because we seek the same coefficient for both $\log R$ and $-\log r$, examining specific relationships between R and r is more effective than applying multiple regression. This approach allows us to understand how different dependencies may affect the calculation of the Assouad dimension.

One of the most widely studied relationships is the exponential form $R = r^\theta$, where $\theta \in (0,1)$. This choice generates the Assouad spectrum, introduced in [12] and defined (for a general set F) by

$$\dim_{\mathrm{A}}{}^{\theta}(F) = \inf\left\{\alpha : \exists C > 0 \text{ such that } \forall\, 0 < r < 1,\ \sup_{x\in F} N_r(B(x,r^\theta)\cap F) \leq C\left(\frac{r^\theta}{r}\right)^{\alpha}\right\}.$$

As shown in [11], for $p > 0$ and $F_p = \{0\} \cup \{1/n^p : n \in \mathbb{N}\}$, the Assouad spectrum satisfies

$$\dim_{\mathrm{A}}{}^{\theta} F_p = \min\left\{\frac{1}{(1-\theta)(1+p)}, \dim_{\mathrm{A}} F_p\right\}.$$

In the proof of Example 1, we use $\theta = 1/2$ and $p = 1$.

For readers interested in the Assouad spectrum and its generalizations, we recommend [1] and [11] for further exploration.

2.3. **Range of R and r.** The finite subset F', used as an approximation of the infinite set F, resembles a real-world fractal in way that it is finite in detail and size, it only resembles the original set F within specific scales. Scale-dependent variations in natural and synthetic fractal structures have been recognized since the early developments in fractal geometry. In fact, Mandelbrot [15] suggested

[1] In [3], the authors examine the time required for an orbit in the chaos game to attain a specified density within the attractor of a strictly contracting iterated function system (IFS), a problem closely related to choosing the appropriate size N. However, their findings indicate that the covering time is dictated by the Minkowski dimension, which we aim to set aside here, as this paper seeks to motivate future work on calculating the Assouad dimension of a set with unknown dimension.

that strict scale invariance is generally valid only within specific, well-defined bounds where particular processes govern structural patterns. However, systematic methods for determining these bounds in real-world structures have not yet been widely developed or applied.

This issue arises because, if r is relatively large compared to R (i.e., if $\frac{R}{r}$ is small), then $N_r(B(x, R) \cap F)$ becomes limited, causing $\log N_r(B(x, R) \cap F)$ to approach an upper bound of $\alpha = 1$. Conversely, when r is very small relative to R (i.e., if $\frac{R}{r}$ is large), $N_r(B(x, R) \cap F)$ is constrained by the finite cardinality of the set F', resulting in $\alpha = 0$. Therefore, the true value of α lies between these extremes, occurring when $\frac{R}{r}$ is neither "excessively large" nor "small".

2.4. **Number of measurements, step for r and R.** The selection of values for r and R significantly impacts both the estimation of α and the computational resources required. For example, fixing $R = r^{1/2}$ and choosing $r = 1/n^2$ for $n \in \mathbb{N}$, as in Example 1, differs markedly from selecting $r = e^{-n}$, which emphasizes measurements at smaller scales, or $r = \varepsilon \cdot n$ for some small ε and n from 1 to $\left[\frac{1}{\varepsilon}\right] + 1$, which provides a uniform step. In all cases, it is unnecessary to let r and R exceed $\operatorname{diam} F' = 1$ or fall below the smallest distance between any two points in the set, given by $\frac{1}{(N-1)(N-2)}$ for $N \geq 4$.

In applied fractal dimension studies (such as [17]), the most common choice for r follows an exponential decay, typically halving with each step. However, this choice is rarely justified in the literature. The most recent rigorous discussion on this selection method (to the best of the authors' knowledge) appears in [7], where the author analyzes particular dimension types (excluding the Assouad dimension) and show that if r follows a geometric sequence, then the slope of the least-squares line can converge to the target dimension. He also notes that when a precise power law describes the fractal, the convergence rate is $O(\log(1/r))$. Despite these insights, this topic has seen limited mathematical investigation since then. For work in related fields, see [16], [14], [5], [4], [13], and [8].

2.5. **Linear regression methodology.** In both ordinary least squares (OLS) and least absolute deviation (LAD) regression, the goal is to fit a line to observed data by minimizing different error metrics: the L_2 norm in OLS and the L_1 norm in LAD. In OLS, the relationship between the independent variable x and the dependent variable y is modeled by the line $y = \beta_0 + \beta_1 x$, with parameters estimated by minimizing the sum of squared residuals, corresponding to the L_2 norm of the residual vector:

$$\min_{\beta_0, \beta_1} |y - (\beta_0 + \beta_1 x)|^2$$

This method is computationally efficient and works well when the data is clean. However, OLS is sensitive to outliers, as large residuals influence the fit. In contrast, LAD minimizes the sum of absolute residuals, corresponding to the L_1 norm:

$$\min_{\beta_0, \beta_1} |y - (\beta_0 + \beta_1 x)|$$

This method is more robust to outliers, as it is less affected by large deviations, making it particularly useful for data with non-constant variance or heavy-tailed distributions. LAD is more computationally expensive and requires iterative optimization methods, but it provides more stable results in the presence of noisy or corrupted data. More about these methods can be found in [6]. For estimating some fractal dimensions (box dimension, correlation dimension, etc. [17]), the OLS method is typically used to model the relationship between $\log N_r(B(x,R)\cap F)$ and $\log \frac{R}{r}$. However, this approach assumes data points are independent, which is often not the case in fractal analysis, where the same object is analyzed at multiple scales. This dependence makes standard regression statistics, such as p-values and confidence intervals, unreliable. Furthermore, the assumption of constant variance and Gaussian-distributed residuals is often violated, as discussed in [13]. In such cases, LAD regression, by minimizing the L_1 norm of the residuals, provides a more robust estimate, especially when data exhibits non-constant variance or heavy tails. By reducing the influence of outliers, LAD is better suited for real-world data, where small measurement errors are common. Given these considerations, both OLS and LAD will be applied in our analysis, with the most appropriate method chosen based on the characteristics of the data and the robustness required for accurate Assouad dimension estimation.

A significant challenge in the estimation of the Assouad dimension, closely related to the selection of the range and step size for R and r, is the global non-linearity of the data. Specifically, for big values of $\frac{R}{r}$, the data plot tends to "curve" toward a slope of 0, resulting in smaller estimates of the parameter α. This issue becomes particularly pronounced when a substantial number of measurements are taken with big values of $\frac{R}{r}$.

This underscores the need to identify the linear region of the data. A rigorous approach to this problem is provided in [9], where all potential slopes derived from various segments of the curve (with lengths greater than a specified minimum) are estimated. These slopes are weighted by their segment length and inverse error, forming a distribution. The mean of this distribution is then taken as the slope estimate, with the quantiles providing confidence intervals. The method was further extended in [10] to include convergence criteria for correlation dimension estimates in certain dynamical systems. However, this algorithm introduces four additional numerical variables, which significantly influence the quality of the fit, making the method challenging to implement. Additionally, the computational complexity of the algorithm is $O(N^2)$ for a relationship curve with N points.

Another key consideration is the potential for over-calculating, or selecting an excessively large number of values for r. The plot of $\log N_r(B(x,R)\cap F)$ versus $\log \frac{R}{r}$ is expected to resemble a step function [2]. Since the objective is to estimate α through linear regression, achieving a linear trend in this plot is essential. Although uniform distribution of data points across the independent variable is not strictly necessary in linear regression, a more even distribution generally enhances the accuracy and efficiency of the regression estimates.

3. Calculations

We address these issues by following a structured approach: first, we vary the set $F' = \{0\} \cup \bigcup_{n=1}^{N-1} \left\{\frac{1}{n}\right\}$ with sizes $N = 100, 200, 300, \ldots, 1000$, constrained by the author's computational resources. Second, we fix the ratio θ of r and R, setting $R = r^{1/2}$. With this, the ratio of R/r equals $r^{-1/2}$. Next, we calculate the maximal range for r and R, ensuring that $\frac{1}{(N-1)(N-2)} \leq r \leq R \leq \operatorname{diam} F' = 1$. Then we vary how r and R approach 0: linearly, exponentially, and by the rational function $\frac{1}{n}$, inspired by the structure of the set itself. Then we count $N_r(B(x, R) \cap F)$ for each r and R. Afterward, we compute the Assouad dimension $\dim_{\mathrm{A}} F'$ as the slope of the line obtained by using both ordinary least squares (OLS) and least absolute deviation (LAD) methods for $\log \frac{R}{r}$ vs. $\log N_r(B(x, R) \cap F')$. Regression analysis is performed on the results, with a focus on predicting the number of points needed to generate F' such that $\dim_{\mathrm{A}} F' = 1$. For this, OLS will be employed, as no outliers are expected in the data, and significant differences between methods are not anticipated. Finally, the effectiveness of each method will be evaluated based on the precision of the calculations and the computational cost, measured by the number of recalculations required.

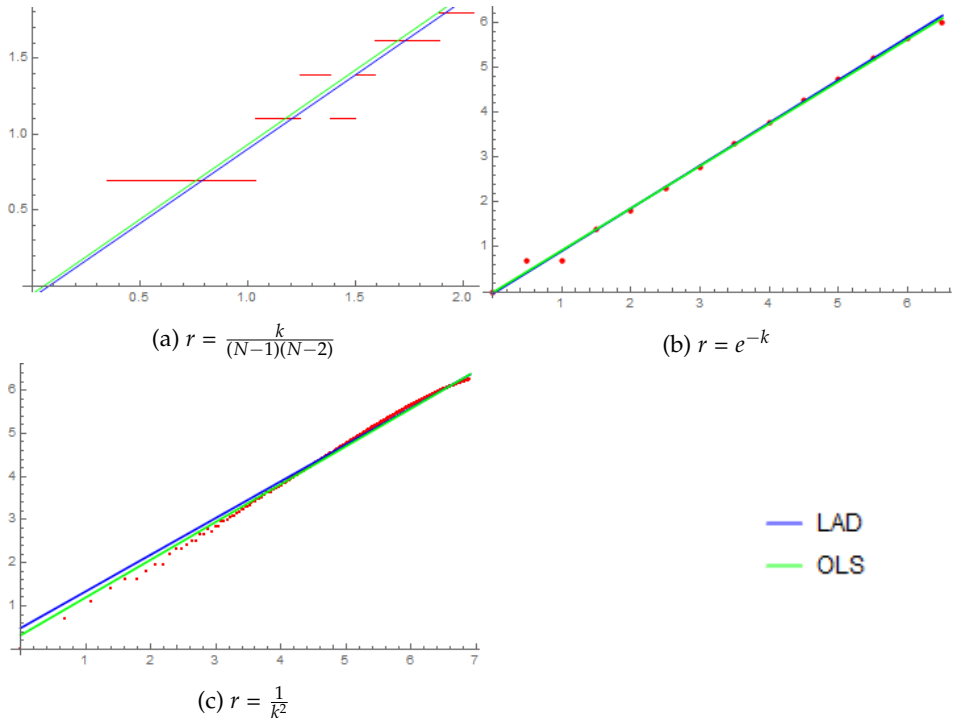

(a) $r = \frac{k}{(N-1)(N-2)}$

(b) $r = e^{-k}$

(c) $r = \frac{1}{k^2}$

FIGURE 1. OLS and LAD fitting for different approaches to 0 with $N = 1000$

N	$r = \frac{k}{(N-1)(N-2)}$	$r = e^{-k}$	$r = \frac{1}{k^2}$
	$k \in \mathbb{N}$ such that $\frac{1}{(N-1)(N-2)} \leq r \leq 1$		
100	0.976709	0.874662	0.829784
200	0.97976	0.905998	0.851313
300	0.980612	0.914583	0.859992
400	0.980958	0.928827	0.865277
500	0.981144	0.925921	0.868571
600	0.981297	0.933554	0.870912
700	0.981385	0.926462	0.872767
800	0.98146	0.933147	0.874168
900	0.981503	0.938238	0.875464
1000	0.981539	0.941662	0.876529

TABLE 1. OLS method calculations for $\dim_{\mathrm{A}} F'$

N	$r = \frac{k}{(N-1)(N-2)}$	$r = e^{-k}$	$r = \frac{1}{k^2}$
	$k \in \mathbb{N}$ such that $\frac{1}{(N-1)(N-2)} \leq r \leq 1$		
100	0.975512	0.87889	0.806391
200	0.97568	0.916291	0.837238
300	0.975661	0.924196	0.848707
400	0.975648	0.936327	0.854226
500	0.975675	0.929913	0.84985
600	0.975686	0.938842	0.852716
700	0.975682	0.944623	0.851638
800	0.975674	0.950273	0.851583
900	0.97568	0.953051	0.851986
1000	0.975675	0.954771	0.851768

TABLE 2. LAD method calculations for $\dim_{\mathrm{A}} F'$

Figure 1 presents the graphical results of OLS and LAD fitting across various approaches of $r \to 0$ with $N = 1000$, where $k \in \mathbb{N}$ such that $\frac{1}{(N-1)(N-2)} \leq r \leq 1$. The x- and y-axes represent $\log \frac{R}{r}$ and $\log N_r(B(x,R) \cap F')$, respectively. Numerical results, obtained by varying N in steps of 100 and examining different approaches for r as it approaches 0, are provided in Tables 1 and 2. These results are summarized in Figure 2 for a graphical representation.

Figure 2 illustrates that for any given N, the best approximation of $\dim_{\mathrm{A}} F$ is achieved when r decreases linearly by a factor of $\frac{1}{(N-1)(N-2)}$, with linear fitting

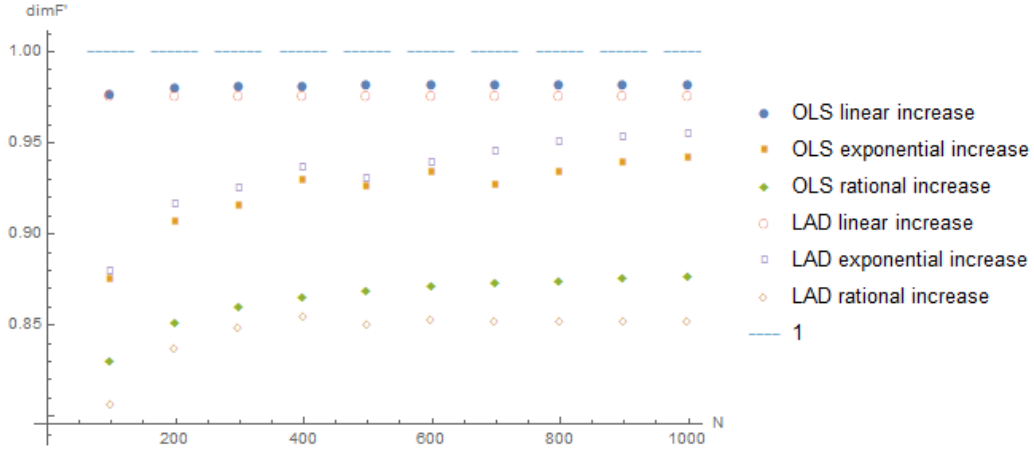

FIGURE 2. Graphical representation of the results in Table 1 and Table 2.

performed using the OLS method. However, this method converges slowly in the long term. The fastest convergence is observed when r decreases exponentially by a factor of e, with linear fitting done using the LAD method.

In Figure 1, the graph of $\log \frac{R}{r}$ versus $\log N_r(B(x,R) \cap F')$ shows the most linear behavior when r approaches 0 exponentially. Additionally, for the uniform approach to 0 with step size $\frac{1}{(N-1)(N-2)}$, the graph is more saturated, indicating a higher number of measurements compared to the other cases. This raises the question: Does increasing the number of measurements with exponentially decaying r lead to a higher approximation of $\dim_A F$?

In Figure 3, we present the results of OLS and LAD fitting for data derived via an exponential decay of r with step sizes $e^{0.1}, e^{0.25}, e^{0.5}, e$, for $N = 1000$, where $k \in \mathbb{N}$ and $\frac{1}{(N-1)(N-2)} \leq r \leq 1$. The x- and y-axes correspond to $\log \frac{R}{r}$ and $\log N_r(B(x,R) \cap F')$, respectively. It is evident that as the step size decreases, the graph becomes more saturated with measurements, resembling a step function. The corresponding numerical results for the OLS method are shown in Table 3, and those for the LAD method in Table 4. A summary of these results is provided in Figure 4.

Figure 4 shows a logarithmic relationship between the number of points N and the Assouad dimension $\dim_A F'$, with similar convergence rates across all methods. By fitting the model $\dim_A F' = a \cdot \log N + b$ using the OLS method and solving $a \cdot \log N + b = 1$ for each step size $(e^{0.1}, e^{0.25}, e^{0.5}, e)$ and method (OLS, LAD), we find that the fastest convergence occurs with the LAD exponential approach to 0 using step size e. However, none of the OLS assumptions were satisfied in any of the models. The model predicts that a fractal generated with 4216 points and measured with $r = e^{-k}$ will have $\dim_A F' = 1$. As shown in Table 4, actual calculations do not align with this prediction. To refine the model, we calculated

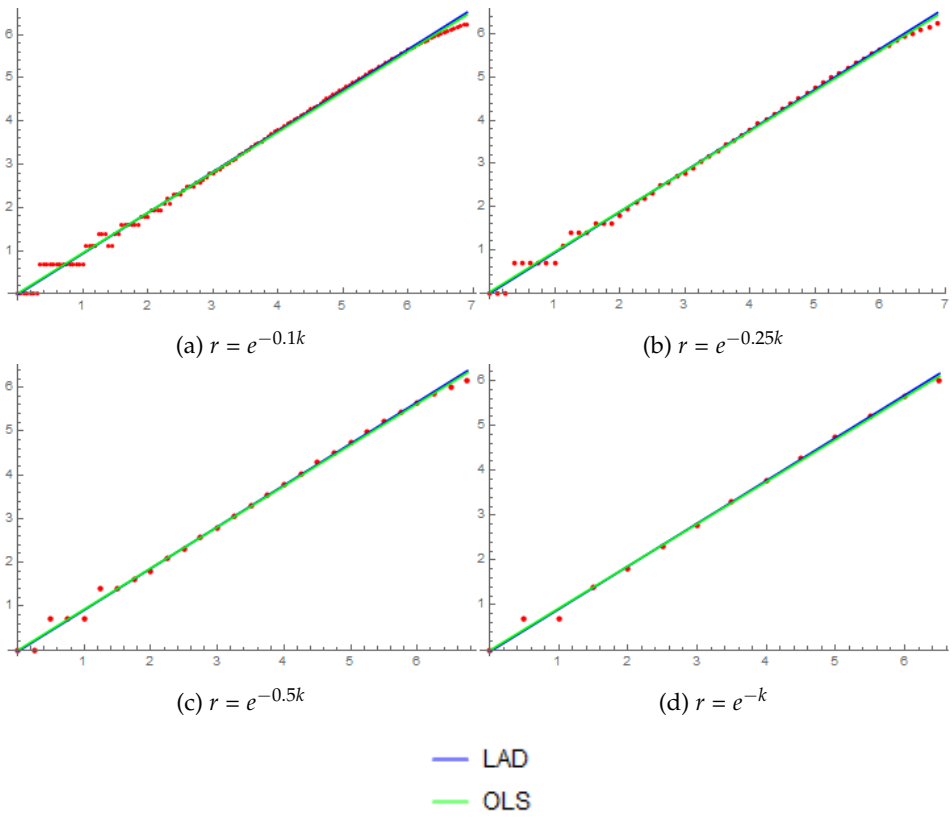

FIGURE 3. OLS and LAD fitting for different exponential approach to 0 with $N = 1000$.

$\dim_A F'$ for N between 100 and 4000 with a step size of 100, as presented in Figure 5. The OLS model exhibits a similar trend.

In Figure 5 we see "dimension drop" at certain N's. The logical reasoning is this: To obtain a finer measurement, it is necessary to increase N sufficiently so that the next smaller r, scaled by a factor of e, fits within the bounds $\frac{1}{(N-1)(N-2)} \leq r \leq 1$. Before this sufficient increase, increasing N only adds points to F' (the number of r's stays the same), this contribute to bigger number of covering balls. This phenomenon is particularly pronounced in the exponential case due to the relatively large step between consecutive r-values. Thus, the dimension drop shown on Figure 5 occurs.

The number of r's that fit within the bounds $\frac{1}{(N-1)(N-2)} \leq r \leq 1$ for different step size is very important for the computational cost. In contrast, when r decreases linearly by a step size of $\frac{1}{(N-1)(N-2)}$, there are $(N-1)(N-2)$ plausible values for r. For $r = \frac{1}{k^2}$, where $k \in \mathbb{N}$, there are only $\lfloor \sqrt{(N-1)(N-2)} \rfloor$ plausible values,

TABLE 3. OLS method calculations for $\dim_A F'$ with exponential approach to 0

N	$r = e^{-0.1k}$	$r = e^{-0.25k}$	$r = e^{-0.5k}$	e^{-k}
	$k \in \mathbb{N}$ such that $\frac{1}{(N-1)(N-2)} \leq r \leq 1$			
100	0.881012	0.880802	0.887282	0.874662
200	0.903406	0.89994	0.906607	0.905998
300	0.914054	0.912203	0.922337	0.914583
400	0.919925	0.919249	0.929029	0.928827
500	0.923647	0.923183	0.931964	0.925921
600	0.928217	0.924277	0.93288	0.933554
700	0.930954	0.927846	0.93215	0.926462
800	0.932933	0.930608	0.938707	0.933147
900	0.933676	0.93231	0.936536	0.938238
1000	0.935524	0.933326	0.940887	0.941662
2000	0.946913	0.944731	0.9482	0.943679
3000	0.949548	0.947249	0.950136	0.946006
4000	0.955332	0.951109	0.953928	0.955625
5000	0.955342	0.95271	0.955341	0.951632
6000	0.957169	0.955574	0.960688	0.957484
7000	0.957566	0.957414	0.959987	0.961452

resulting in significantly lower computational demand. When r decays exponentially as $r = e^{-k}$, the number of plausible values for r is $\lfloor \ln (N-1)(N-2) \rfloor$, making the exponential decay the most computationally efficient. For instance, even with $r = e^{-0.1k}$, the number of measurements is just $10\lfloor \ln (N-1)(N-2) \rfloor$ which is significantly lower than $(N-1)(N-2)$, therefore reducing the computational burden.

For example, for $N = 100$, the number of r's fitting within the bounds $\frac{1}{(N-1)(N-2)}$ to 1 is 9702 for the linear approach, 98 for the $\frac{1}{k^2}$ approach, and only 9 for the exponential decay (step e) approach. To achieve approximately 10,000 measurements with the exponential (step e) approach, N would need to be around 2.97×10^{2171}, which highlights the practical limitations of such an approach, even for relatively simple fractals.

It is important to note that the code, written in Wolfram Mathematica, avoids rounding errors when working with fractions, ensuring exact precision in all calculations. This feature is crucial for handling complex fractal computations without introducing inaccuracies, especially when dealing with very small or large values.

TABLE 4. LAD method calculations for $\dim_{\mathrm{A}} F'$ with exponential approach to 0

N	$r = e^{-0.1k}$	$r = e^{-0.25k}$	$r = e^{-0.5k}$	e^{-k}
	$k \in \mathbb{N}$ such that $\frac{1}{(N-1)(N-2)} \leq r \leq 1$			
100	0.876712	0.867301	0.881171	0.87889
200	0.905281	0.914064	0.919679	0.916291
300	0.918919	0.92773	0.928393	0.924196
400	0.925855	0.932688	0.934186	0.936327
500	0.93204	0.932922	0.934453	0.929913
600	0.93852	0.937107	0.944256	0.938842
700	0.94046	0.940363	0.942339	0.944623
800	0.943083	0.941032	0.947559	0.950273
900	0.944016	0.942339	0.94819	0.953051
1000	0.947252	0.946631	0.951141	0.954771
2000	0.959129	0.957135	0.961463	0.957498
3000	0.962607	0.962928	0.963398	0.958727
4000	0.970105	0.966093	0.965589	0.965589
5000	0.968846	0.968147	0.967333	0.968055
6000	0.971156	0.968428	0.973581	0.968055
7000	0.971813	0.972026	0.970711	0.969642

4. CONCLUSION

With fixed $R = r^{1/2}$ for the fractal $F = \{0\} \cup \{1/n : n \in N\}$, the **linear decay of r with the OLS method**, where the step is $\frac{1}{(N-1)(N-2)}$, consistently yields the most accurate estimation of the Assouad dimension $\dim_A F'$ across all values of N. Although the **exponential decay of** r (where $r = e^{-k}$) results in faster convergence, the **linear decay method** consistently provides superior precision in approximating the Assouad dimension at any given N.

The **exponential decay** of r reduces computational requirements by requiring fewer measurements; however, this comes at the cost of decreased precision, regardless of whether OLS or LAD is used. Among the methods utilizing exponential decay, the LAD method offered improved precision in approximating the Assouad dimension.

In contrast, the **linear decay method**, while computationally more demanding, produces more reliable estimates of $\dim_A F'$ due to its consistent accuracy across N. Furthermore, within the linear decay approach, no significant difference in performance was observed between the OLS and LAD fitting methods.

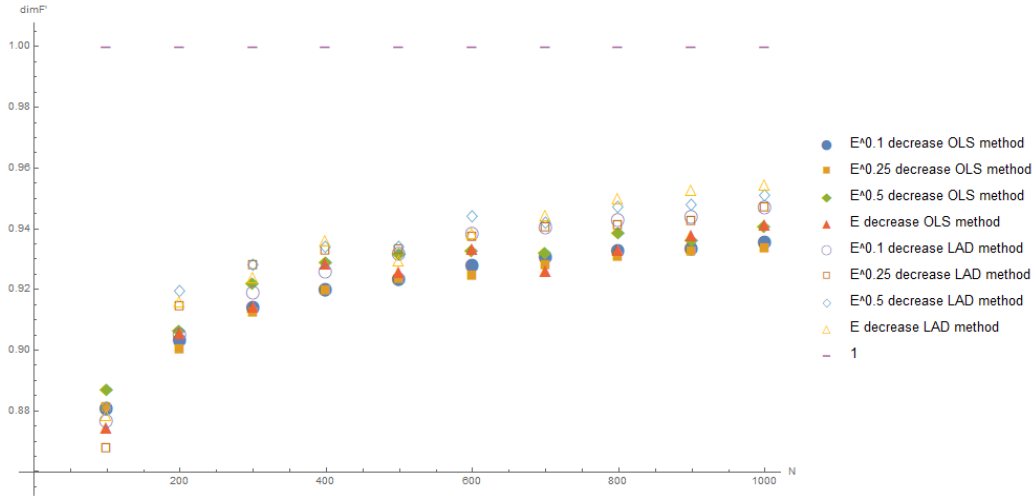

FIGURE 4

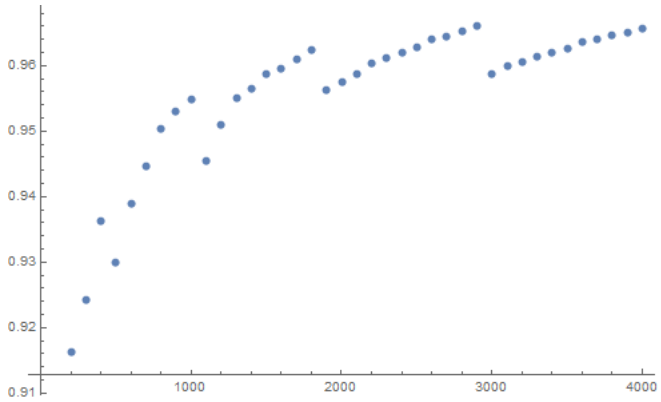

FIGURE 5. LAD exponential approach to 0 with step reduction of e where the x and y axis correspond to N and $\dim_A F'$.

The author would like to express their gratitude to Sascha Troscheit, Sonja Gegovska-Zajkova, and Katerina Hadzhi-Velkova Saneva for their valuable feedback on an earlier version of this document, and to Risto Chavdarov for providing the system support necessary for the calculations.

REFERENCES

[1] A. Banaji, A. Rutar, S. Troscheit, *Interpolating with generalized Assouad dimensions*, arXiv:2308.12975 (2023).

[2] M. F. Barnsley, *Fractals Everywhere*, Dover Publications, Inc., USA, 2012.

[3] B. Bárány, N. Jurga, I. Kolossváry, *On the Convergence Rate of the Chaos Game*, International Mathematics Research Notices, 2023 (5), Oxford University Press (2022) 4456–4500.

[4] G. M. Berntson, P. Stoll, *Correcting for finite spatial scales of self–similarity when calculating fractal dimensions of real–world structures*, Proceedings of the Royal Society of London. Series B: Biological Sciences, 264 (1531), Royal Society Publishing (1997) 1531–1537.

[5] M. Bouda, J. S. Caplan, J. E. Saiers, *Box-Counting Dimension Revisited: Presenting an Efficient Method of Minimizing Quantization Error and an Assessment of the Self-Similarity of Structural Root Systems*, Frontiers in Plant Science, 7 (149), 2016, https://doi.org/10.3389/fpls.2016.00149.

[6] K. Chen, Z. Ying, H. Zhang, L. Zhao, *Analysis of least absolute deviation*, Biometrika, 95 (1), 2008, 107–122, doi:10.1093/biomet/asm082.

[7] C. D. Cutler, *Some results on the behavior and estimation of the fractal dimensions of distributions on attractors*, Journal of Statistical Physics, 62, Springer (1991) 651–708, https://doi.org/10.1007/BF01017978.

[8] G. Datseris, I. Kottlarz, A. P. Braun, U. Parlitz, *Estimating fractal dimensions: A comparative review and open source implementations*, Chaos: An Interdisciplinary Journal of Nonlinear Science, 33 (10), AIP Publishing (2023), https://doi.org/10.1063/5.0160394.

[9] V. Deshmukh, E. Bradley, J. Garland, J. D. Meiss, *Toward automated extraction and characterization of scaling regions in dynamical systems*, Chaos: An Interdisciplinary Journal of Nonlinear Science, 31 (12), AIP Publishing (2021), https://doi.org/10.1063/5.0069365.

[10] V. Deshmukh, R. Meikle, E. Bradley, J. D. Meiss, J. Garland, *Using scaling-region distributions to select embedding parameters*, Physica D: Nonlinear Phenomena, 446, Elsevier (2023) 133674, https://doi.org/10.1016/j.physd.2023.133674.

[11] J. M. Fraser, *Assouad Dimension and Fractal Geometry*, Cambridge University Press, Cambridge, 2020.

[12] J. M. Fraser, H. Yu, *New dimension spectra: Finer information on scaling and homogeneity*, Advances in Mathematics, 329, Elsevier (2018) 273–328, https://doi.org/10.1016/j.aim.2017.12.019.

[13] J. M. Halley, S. Hartley, A. S. Kallimanis, W. E. Kunin, J. J. Lennon, S. P. Sgardelis, *Uses and abuses of fractal methodology in ecology*, Ecology Letters, 7 (3), 2004, 254–271, doi:10.1111/j.1461-0248.2004.00568.x.

[14] W. Jiang, Y. Liu, J. Wang, R. Li, X. Liu, J. Zhang, *Problems of the Grid Size Selection in Differential Box-Counting (DBC) Methods and an Improvement Strategy*, Entropy, 24 (7), MDPI (2022) 977, https://doi.org/10.3390/e24070977.

[15] B. B. Mandelbrot, *The Fractal Geometry of Nature*, Henry Holt and Company, 1983.

[16] E. Rosenberg, *Fractal Dimensions of Networks*, Springer, Cham, 2020, https://doi.org/10.1007/978-3-030-43169-3.

[17] H. Tong, *Dimension Estimation and Models*, World Scientific, Singapore, 1993.

JASMINA ANGELEVSKA KOSTADINOSKA
SS. CYRIL AND METHODIUS UNIVERSITY,
FACULTY OF ELECTRICAL ENGINEERING AND INFORMATION TECHNOLOGIES,
RUGJER BOSHKOVIKJ, SKOPJE 1000, NORTH MACEDONIA
Email address: jasminaa@feit.ukim.edu.mk

Received 15.11.2024
Revised 07.12.2024
Accepted 24.12.2024